



Blur Invariant Template Matching Using Projection onto Convex Sets

Matěj Léb1^(✉), Filip Šroubek¹, Jaroslav Kautský², and Jan Flusser¹

¹ Institute of Information Theory and Automation, The Czech Academy of Sciences,
Pod Vodárenskou věží 4, 182 08 Prague 8, Czech Republic
{lebl,sroubek,flusser}@utia.cas.cz

² The Flinders University of South Australia, Adelaide, Australia

Abstract. Blur is a common phenomenon in image acquisition that negatively influences recognition rate if blurred images are used as a query in template matching. Various blur-invariant features and measures were proposed in the literature, yet they are often derived under conditions that are difficult to satisfy in practise, for example, images with zero background or periodically repeating images and classes of blur that are closed under convolution. We propose a novel blur-invariant distance that puts no limitation on images and is invariant to any kind of blur as long as the blur has limited support, non-zero values and sums up to one. A template matching algorithm is then derived based on the blur-invariant distance, which projects query images on convex sets constructed around template images. The proposed method is easy to implement, it is robust to noise and blur size, and outperforms other competitors in this area.

Keywords: Blur-invariant distance · Projection operator · Object recognition · Blurred image

1 Introduction

Image recognition covers a wide variety of practical and theoretical areas ranging from feature-based classification for product quality control to complex tasks such as video tracking used in forensics. The images themselves vary not only in captured information but also in quality. This paper focuses on a recognition of blurred templates. We introduce a method that can match a blurred query image against a database of clean templates. This task is very challenging as the templates may be fairly similar and some inputs can be severely degraded so that visual recognition is difficult. Presented results thus serve not only as automation of the recognition process but also help in cases when human visual classification fails.

This work was supported by the Czech Science Foundation (Grant No. GA18-07247S) and by the Praemium Academiae, awarded by the Czech Academy of Sciences.

© Springer Nature Switzerland AG 2019
M. Vento and G. Percannella (Eds.): CAIP 2019, LNCS 11678, pp. 351–362, 2019.
https://doi.org/10.1007/978-3-030-29888-3_28

A commonly used model of image acquisition is a simple convolution equation

$$g = f * h + n, \quad (1)$$

where f is the ideal original image, h is the blur kernel representing the degradation, and n is noise. Although this model is only an approximation of the real image formation process, it is a reasonable and mathematically tractable simplification of many real scenarios. In this paper, we assume the image degradation (blur and noise) to follow the model (1).

Since 1960's, a large number of papers have been devoted to image restoration, i.e. to estimation of f from its blurred version g . This is, however, superfluous for template matching purposes. One can avoid the time-consuming and ill-posed inversion of (1) by designing a matching algorithm, which is robust (or even totally invariant) to the blur. In this paper, we propose a new algorithm of this kind.

We show that all admissible blurred versions of an image form a convex set in the image space. We construct this set for each database template f_i . Given a query image g , we measure its distance to all these convex sets and g is then classified by a minimum distance rule. We show that the distance between an image and a convex set is a simple minimization problem which can be efficiently resolved numerically. This results in a blur-invariant matching algorithm, which outperforms state-of-the-art methods in most aspects. The performance of the algorithm is illustrated by experiments on standard datasets of human faces and handwritten digits.

The paper is organized as follows. First, we give an overview of related work in Sect. 2 and then we formulate the proposed blur-invariant distance formally in Sect. 3. The presented theory is used for developing a projection based method for blur-invariant template matching in Sect. 4. Sections 5 and 6 discuss the effect of noise and the blur size. Finally, the experimental Sect. 7 verifies the theory and provides a comparison with three reference methods.

2 Related Work

Methods performing the blur-invariant image recognition task can be categorized according to assumptions on the blur kernel properties. Most of the methods assume a particular shape of the blur and then construct invariants to convolution with the kernel of this kind. Classification is then performed in the space of invariants, usually by the minimum distance rule [8]. This approach was originally introduced by Flusser et al. [5, 7] who proposed moment-based invariants w.r.t. centrosymmetric blur. Later on, their theory was extended to N -fold symmetric blur [6, 15] and N -fold dihedral blur [16].

If a parametric form of the blur kernel is known, the invariants from the above group do not provide a maximum possible discrimination power because they do not employ the parametric form explicitly. In order to maximize the discriminability, some authors attempted to design special blur invariants w.r.t. rotation-symmetric Gaussian blur. First invariants of this kind were found

heuristically [13,17] but recently a consistent theory of Gaussian blur invariants was presented in [4]. An interesting method, still limited to Gaussian blur, was published by Zhang et al. [20]. Instead of deriving blur invariants explicitly, the authors proposed a distance measure between two images which is independent of circular Gaussian blur. Their core idea is to estimate the blur level of images to be compared, bring them to the same blur level by blurring of the one which is less blurred, and then measure their similarity by the geodesic distance on a manifold.

Gopalan et al. [10] derived another blur-invariant distance measure without assuming the knowledge of the blur shape but imposed a limitation on its support size. From this point of view, their method is the closest one to our proposed technique, so we review their method in more detail.

Gopalan et al. established the correspondence between images and subspaces representing points on Grassmann manifold. Classification is then performed by minimizing the Riemannian distance of those points. This distance can be viewed as measuring angles between two subspaces. Gopalan et al. consider \mathcal{H} to be a set of *arbitrary* blur kernels with fixed support $m \times n$, i.e.

$$\mathcal{H} = \{h \in (\mathbb{R})^{m \times n}\}. \tag{2}$$

Then any blur $h \in \mathcal{H}$ can be written as a linear combination of “basis” blurs. Without loss of generality we can consider the standard basis

$$h_{ij}(x, y) = \begin{cases} 1, & \text{if } x = i, y = j, \\ 0, & \text{otherwise} \end{cases} \tag{3}$$

where $i = 1, \dots, m, j = 1, \dots, n$. The basis blurs are thus shifted delta functions.

Let us denote the set of all images resulting from the convolution of clear image f with the basis blurs h_{ij} as

$$\mathcal{S}_f = \{f * h_{ij}, i = 1, \dots, m, j = 1, \dots, n\}. \tag{4}$$

Consequently, the blur invariance of $\text{Span}(\mathcal{S}_f)$ is proven, i.e. $\text{Span}(\mathcal{S}_f) = \text{Span}(\mathcal{S}_g)$. In theory, when g is a blurred version of f , both subspaces $\text{Span}(\mathcal{S}_f)$ and $\text{Span}(\mathcal{S}_g)$ are identical. Employing Grassmann manifold recognition is then performed by means of the minimum-distance classifier with metric defined by Riemannian distance $d_G(\text{Span}(\mathcal{S}_g), \text{Span}(\mathcal{S}_f))$.

3 Blur-Invariant Distance

Blur functions in standard acquisition scenarios have various shapes, yet typically they have three properties in common: limited support, non-negative values, and preservation of the mean image intensity. Let us define the set of admissible blurs with these properties as

$$\mathcal{H} := \left\{ h \in (\mathbb{R})^{m \times n} \mid h(x, y) \geq 0, \sum_{x,y} h(x, y) = 1 \right\}. \tag{5}$$

where $D = m \times n$ is the maximal assumed blur size. Note that imposing the non-negativity and brightness-preservation constraints is a significant difference from the assumptions used in [10], which changes the geometry of blur-invariant sets. We will now derive a blur-invariant distance with respect to \mathcal{H} .

The set of blurs \mathcal{H} in (5) is a convex set with D vertices. For every image f of size N , the set of all its blurred versions

$$\mathcal{C}_f := \left\{ f * h \mid h \in \mathcal{H} \right\} \tag{6}$$

is also a convex set residing in the N dimensional space, which follows from linearity of convolution. The convex set is equivalent to a convex hull of \mathcal{S}_f in (4). By definition, $g \in \mathcal{C}_f \Leftrightarrow g = h * f$ for some $h \in \mathcal{H}$. The blur invariant matching problem can be therefore seen as a task to find, for query image g , the closest set \mathcal{C}_f .

Let us denote the projection of g onto \mathcal{C}_f as $P_f(g)$, then

$$I(f, g) := \|P_f(g) - g\| \tag{7}$$

is a blur-invariant distance with respect to \mathcal{H} defined in (5). The projection $P_f(g)$ is a point in \mathcal{C}_f with the shortest Euclidean distance from g . Then the blur-invariant distance can be formulated as minimization

$$I(f, g)^2 = \min_h \|f * h - g\|^2, \text{ s.t. } h \in \mathcal{H}, \tag{8}$$

which is a simple convex problem. If h^* denotes the minimizer of (8), then the projection to \mathcal{C}_f is implemented as $P_f(g) = f * h^*$. The efficient computation of $I(f, g)$ is discussed in Sect. 4.

Due to sampling, quantization and additive noise, $I(f, g)$ might be non-zero even if g is a blurred version of f . In the case of multiple templates $\{f_i\}$, the distance $I(f_i, g)$ is used to determine the closest matching template f^* . The discriminability of this approach is influenced by mutual position and shape of convex sets \mathcal{C}_{f_i} 's, which are determined by the type of template images and the dimension D of \mathcal{H} . An illustration is provided in Fig. 1.

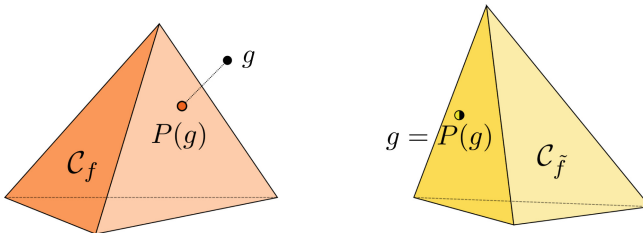


Fig. 1. Illustration of projection process with g not belonging to the convex set \mathcal{C}_f (left) and g being in the set $\mathcal{C}_{\tilde{f}}$.

The proposed blur-invariant distance in (7) has a single parameter, which is the assumed blur size D . In many practical applications, the upper bound of the blur size is known or can be estimated. In addition, the distance is robust to size overestimation as discussed in Sect. 6 and to some extent also to underestimation as shown in Sect. 7.

Simple visualization of main differences between Zhang’s, Gopalan’s and ours blur invariant measures is illustrated in Fig. 2.

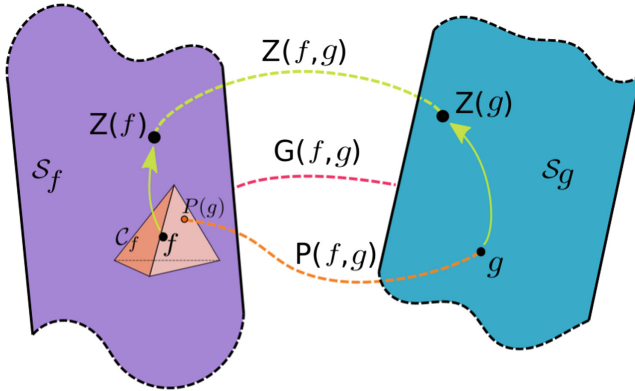


Fig. 2. Illustration of blur invariant distances: Zhang’s (Z) image to image, Gopalan’s (G) subspace to subspace and proposed (P) image to convex set.

4 Implementation Details

The computation of the proposed blur-invariant distance (8) can be formulated as a problem of quadratic programming. Having the given blur set \mathcal{H} with the blur size $D = m \times n$, we first construct for each template image f_i of size $N = k \times l$ a matrix $\mathbf{U}_{f_i} \in \mathbb{R}^{N \times D}$ by vectorizing elements of S_{f_i} and concatenating them, i.e.

$$\mathbf{U}_{f_i} = [\mathbf{F}_i \mathbf{h}_{11}, \dots, \mathbf{F}_i \mathbf{h}_{mn}], \tag{9}$$

where $\mathbf{F}_i \mathbf{h}_{(\cdot, \cdot)}$ is the column vectorized $f * h_{(\cdot, \cdot)}$. Matrices \mathbf{U}_{f_i} are stored and used repeatedly for the same dataset and blur size D . The computational cost is fairly low. For example for the standard basis (3), the columns are just shifted versions of f_i .

The query image g in its vectorized form \mathbf{g} is then used to solve the quadratic problem

$$I(f_i, g)^2 = \min_{\mathbf{h}} \mathbf{h}^T \mathbf{U}_{f_i}^T \mathbf{U}_{f_i} \mathbf{h} - 2\mathbf{g}^T \mathbf{U}_{f_i} \mathbf{h} + \mathbf{g}^T \mathbf{g}, \tag{10}$$

subject to

$$\mathbf{h} \geq 0, \sum \mathbf{h} = 1. \tag{11}$$

The complete algorithm for blur invariant template matching can be described as follows:

1. Prepare the convex set \mathcal{C}_{f_i} for each template image f_i by constructing \mathbf{U}_{f_i} as in (9).
2. For the given query image g and every set \mathcal{C}_{f_i} , compute the blur-invariant distance $I(f_i, g)$ according to (10).
3. The best matching template f^* is $f^* = f_j$, where $j = \arg \min_i I(f_i, g)$.

Note that by solving (10), we obtain the estimated blur h^* as a byproduct, yet our goal is not to restore the query image g . Full recovery of image f is an ill-posed problem even with the knowledge of h ; see e.g. [1, 3, 18, 19]. Here the aim is to find the template, from which the query image was created by degradation.

5 Constraints Versus Noise

Let us consider a query image g that is a blurred version of some template image f , i.e. $g = \tilde{h} * f$, $\tilde{h} \in \mathcal{H}$. In the noiseless case, the minimizer h^* of (8) clearly corresponds to \tilde{h} . In the presence of noise, the acquisition model follows (1) and the minimizer h^* will partially compensate for the introduced noise.

Combining (1) and (8), we obtain

$$\begin{aligned} h^* &= \min_h \|f_i * h - f_i * \tilde{h} - n\|^2 = \\ &= \min_h \|f_i * (h - \tilde{h}) - n\|^2 \end{aligned}$$

and the optimal h^* can be written as

$$h^* = \tilde{h} + c, \quad (12)$$

where

$$c = \arg \min_h \|f_i * h - n\|^2, \quad \text{s.t. } h \in \mathcal{H}$$

The element c serves as a compensation for noise n . The problem is, that noise is Gaussian-distributed, hence c and consequently h^* would be very likely a better minimizer if allowed to have negative values.

Solution to this is to ignore the constraints (11). The quadratic problem in (10) then simplifies to the classical least squares method that is solved by a system of linear algebraic equations as $I(f, g) = \|\mathbf{U}_f(\mathbf{U}_f^T \mathbf{U}_f)^{-1} \mathbf{U}_f^T \mathbf{g} - \mathbf{g}\|$.

Omitting the constraints of blur model (11) means, that we are projecting g onto $\text{Span}(\mathcal{S}_f)$ instead of convex set \mathcal{C}_f . On one hand, this can improve classification of noisy images, on the other hand, we loose some discrimination power. As shown in Sect. 7, there are real-life inspired datasets where the constrained version outperforms the unconstrained one. Figure 3 illustrates the difference between projecting g onto \mathcal{C}_f and $\text{Span}(\mathcal{S}_f)$.

To combine benefits of both versions, we propose to relax the non-negativity constraint but still to keep the brightness-preservation constraint. There are many possibilities how to achieve that. One way is to introduce a penalization for attaining negative value in the minimization problem (10). Other option, which is even simpler, is to change $h \geq 0$ to $h > -\varepsilon$, where ε becomes a new parameter

in the algorithm. During experiments, this approach proved to improve results though the change was not significant and choosing incorrect ε could worsen the recognition rate.

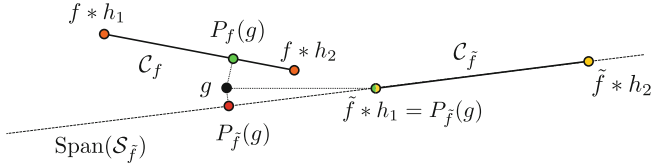


Fig. 3. Simple 2D schematic showing impact of constraints on classification. Convex sets C_f and $C_{\tilde{f}}$ are two line segments. With constraints in effect, $g = f * h + n$ is assigned to the template image f as $\|g - P_f\|^2 < \|g - P_{\tilde{f}}\|^2$. Without the non-negativity constraint, $\|g - P_{\tilde{f}}\|^2$ becomes smaller than $\|g - P_f\|^2$ and \tilde{f} would be incorrectly selected.

Depending on the task we are solving and given set of templates, we have to decide, whether we want to solve unconstrained problem (10) and have better robustness to noise or if we employ constraints (11) and have potentially better results for templates whose convex sets are close together.

6 Blur Size

The main advantage of our method is its generality. We are not bound by any specific blur class and it does not require any input parameters except the blur size. We may attempt to estimate the blur size from given data as described, e.g., in [2] and [14]. This could lead to different blur size settings for each query image even though they were all acquired the same way and its safe to assume that the actual blur support is the same for all of them. Such case would mean unnecessary computational cost.

First, let us discuss the influence of overestimating blur size. It follows immediately from the construction of convex sets and the matrix form of the minimization problem (10) that estimated blur will be the original blur padded with zeroes. Overestimation thus has a negligible effect on the recognition rate and only increases the computational cost since blur size determines the dimension of the problem (10).

We conducted an experiment to quantify the effect of underestimating blur size. Results show (see Fig. 6), that even with over 30% underestimation, the classification still maintains good performance. For most cases it is sufficient to estimate the blur size only once for each given dataset of templates.

7 Experiments

We prepared two datasets, the first one consisting of handwritten binary digits (0–9) from MNIST database [12] and the second one consisting of 38 faces from

YaleB database [9]. We corrupted all images by blur of various sizes and two types – motion (M) and Gaussian blur (G) – and added Gaussian white noise with SNR ranging from 50 dB to 1 dB (see Fig. 4). We compared the proposed projection method (PM) with the method of Gopalan (GM), Zhang (ZM) and with moment-based blur invariants (MI). Two types of moment invariants were used depending on the considered blur. For motion blur, invariants to centrosymmetric blur [5] and for Gaussian blur, invariants to Gaussian blur [11] were used to ensure optimal performance. In all cases, the maximum order of moments was manually tuned to produce the best results. To mimic realistic usage of tested methods, we normalized both template and query images to have unit mean value. This makes recognition generally more difficult but it is necessary in practice.

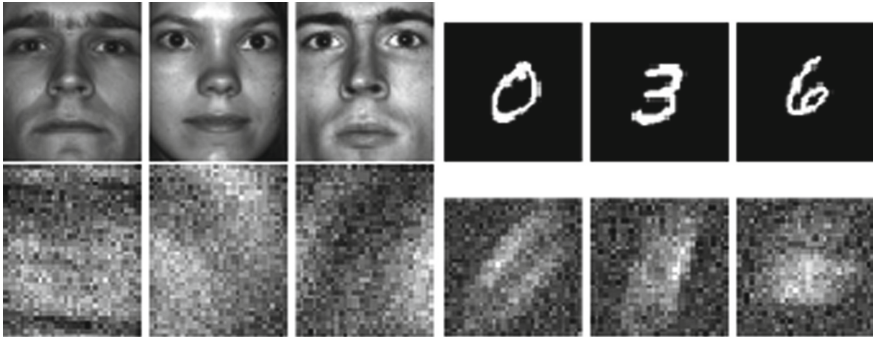


Fig. 4. Examples of the face and digit images used in experiments: clear database (top row) and corrupted query images (bottom).

Tables 1 and 2 summarize the success rate of the classification with changing SNR and blur size, respectively. Compared to the other methods, the proposed method shows excellent robustness to noise, type of the blur and also to the amount of blur. Only in the case of Gaussian blur, MI slightly outperforms the proposed method. This is probably because the MIs were designed specifically for Gaussian blur, while our projection method does not employ any assumption about the kernel parametric form. However in the case of motion blur, small discretization effects break the centrosymmetry assumption and the performance of MI starts to deteriorate. Zhang’s method performs better for Gaussian blur as it is derived for this type of blur. Maybe surprisingly Gopalan’s method shows a relatively poor recognition rate. By construction, it is less dependent on the type of blur compared to the Zhang and MI. Our hypothesis is that the Riemannian distance between often overlapping subspaces is not a good blur-invariant measure.

We compared the performance of all methods using regular desktop PC. Time required for one query-template comparison was measured, results are shown in Fig. 5. Gopalan’s method was implemented based on the “Algorithm 1” in [10] using CS decomposition which is very slow. The time for computing

MI is affected also by the maximum order of moments computed. The highest order used in the previous experiment was used for measuring the computational time. Note that the moment-based algorithm is independent of blur size and the computational time is not affected by it. With increasing image and blur size, MI becomes more time efficient. It outperforms the Projection method for images 600×60 px with blur 50×50 px.

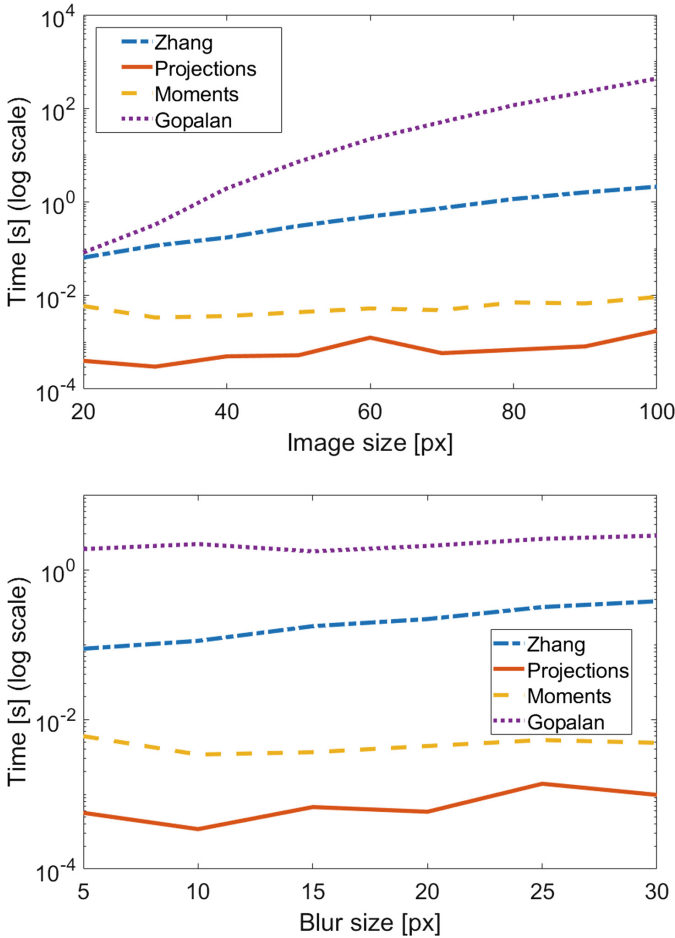


Fig. 5. Time [s] needed to compare one query image to one template: (top) dependency on image size with fixed blur size of 15×15 px and (bottom) dependency on blur size with fixed image size 40×40 px. The Y axis is shown in logarithmic scale.

The graph in Fig. 6 shows that even when we estimate the blur support to be less than 70% of the original one, we still achieve perfect accuracy with the proposed method. For this experiment we used uniform blur as it is the worst possible scenario for underestimated support.

We also tested our hypothesis from Sect. 5, that omitting the non-negativity constraint improves recognition results for noisy images and repeated the experiment for the projection method without the non-negativity constraint. For brevity, we refer to this method as the unconstrained variant and to the original projection method as the constrained variant. For low-level noise, both variants perform the same. However for SNR <5 dB, the constrained variant starts to misclassify query images slightly more often.

Table 1. The recognition rate [%], digits dataset was used with image size 28×28 px and blur size 15×15 px.

SNR [dB]	GM (G)	ZM (G)	MI (G)	PM (G)	GM (M)	ZM (M)	MI (M)	PM (M)
50	99	100	100	100	100	94	100	100
20	67	96	100	100	98	80	99	100
10	45	28	100	100	81	23	85	100
5	38	28	100	98	58	22	79	100
1	35	27	97	86	55	18	53	96

Table 2. The recognition rate [%], faces dataset was used with image size 40×35 px and SNR 20 dB.

Blur size	GM (G)	ZM (G)	MI (G)	PM (G)	GM (M)	ZM (G)	MI (M)	PM (M)
7×7	74	100	100	100	99	100	87	100
11×11	25	86	100	100	76	72	71	100
15×15	5	48	95	100	40	17	45	100

The second experiment demonstrates the opposite scenario when the constrained variant outperforms the unconstrained one. A special dataset was prepared that consists of the same handwritten digits as in the first experiment, but this time we added a frame – either a circle or a square. This was motivated by a problem of traffic-sign recognition where the actual shape of the frame changes the meaning of the sign and it is thus important to correctly match not only the symbol (number), but the frame as well. Sample images are shown in Fig. 7.

Images of size 41×41 px were degraded by motion blur of size 25×25 px and noise with SNR 5 dB was added. The constrained variant maintained 100% recognition accuracy while the unconstrained variant achieved only 85% accuracy. In all the failure cases, the unconstrained algorithm matched the query image with a template containing the correct symbol but a wrong frame. This is in accordance with the illustration in Fig. 3.

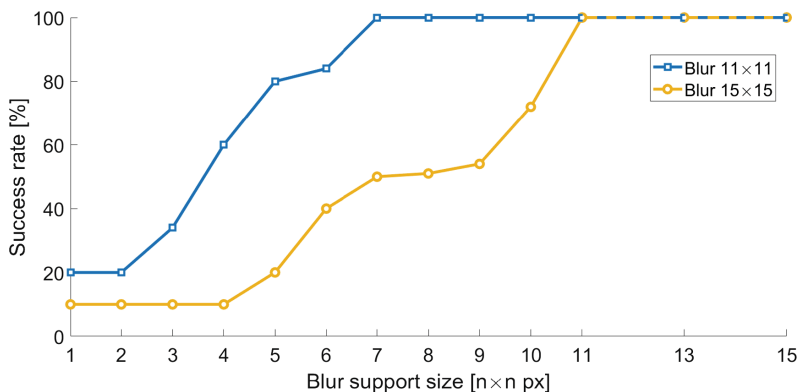


Fig. 6. The recognition rate [%] of projection method w.r.t. underestimation of blur support. Digits dataset was used with uniform blur of size 11×11 (blue) and 15×15 (yellow), both with SNR = 20 dB. (Color figure online)

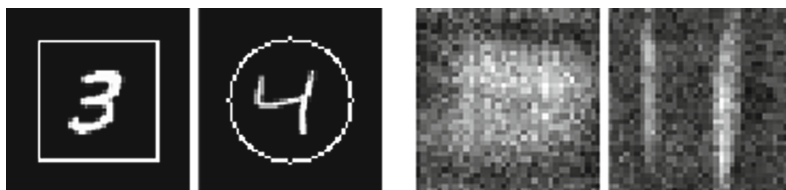


Fig. 7. Example of clean images (left) and their degraded versions (right) used to test the effect of the constrains in the projection method.

8 Conclusion

We showed that the projection onto a convex set representing the template image with its all admissible blurred variants can be used to construct blur-invariant measure for arbitrary blur of finite support. Experiments demonstrated high robustness and recognition rate on a par with the state-of-the-art method of moment invariants while providing better generality. The proposed method is easy to implement and requires only one parameter, which is the maximum expected blur size. A possible future improvement to the proposed method is to introduce regularization in the optimization problem.

References

1. Carasso, A.S.: The APEX method in image sharpening and the use of low exponent Lévy stable laws. *SIAM J. Appl. Math.* **63**(2), 593–618 (2003)
2. Chen, L., Yap, K.H.: Identification of blur support size in blind image deconvolution. In: *Proceedings of the 2003 Joint Fourth International Conference on Information, Communications and Signal Processing and the Fourth Pacific Rim Conference on Multimedia*, vol. 1, pp. 503–507. IEEE (2003)

3. Elder, J.H., Zucker, S.W.: Local scale control for edge detection and blur estimation. *IEEE Trans. Pattern Anal. Mach. Intell.* **20**(7), 699–716 (1998)
4. Flusser, J., Farokhi, S., Höschl IV, C., Suk, T., Zitová, B., Pedone, M.: Recognition of images degraded by Gaussian blur. *IEEE Trans. Image Process.* **25**(2), 790–806 (2016)
5. Flusser, J., Suk, T.: Degraded image analysis: an invariant approach. *IEEE Trans. Pattern Anal. Mach. Intell.* **20**(6), 590–603 (1998)
6. Flusser, J., Suk, T., Boldyš, J., Zitová, B.: Projection operators and moment invariants to image blurring. *IEEE Trans. Pattern Anal. Mach. Intell.* **37**(4), 786–802 (2015)
7. Flusser, J., Suk, T., Saic, S.: Recognition of blurred images by the method of moments. *IEEE Trans. Image Process.* **5**(3), 533–538 (1996)
8. Flusser, J., Suk, T., Zitová, B.: *2D and 3D Image Analysis by Moments*. Wiley, Chichester (2016)
9. Georghiades, A., Belhumeur, P., Kriegman, D.: From few to many: illumination cone models for face recognition under variable lighting and pose. *IEEE Trans. Pattern Anal. Mach. Intell.* **23**(6), 643–660 (2001)
10. Gopalan, R., Turaga, P., Chellappa, R.: A blur-robust descriptor with applications to face recognition. *IEEE Trans. Pattern Anal. Mach. Intell.* **34**(6), 1220–1226 (2012)
11. Kostková, J., Flusser, J., Lébl, M., Pedone, M.: Image invariants to anisotropic Gaussian blur. In: Felsberg, M., Forssén, P.-E., Sintorn, I.-M., Unger, J. (eds.) *SCIA 2019. LNCS*, vol. 11482, pp. 140–151. Springer, Cham (2019). https://doi.org/10.1007/978-3-030-20205-7_12
12. LeCun, Y., Cortes, C.: MNIST handwritten digit database (2010). <http://yann.lecun.com/exdb/mnist/>
13. Liu, J., Zhang, T.: Recognition of the blurred image by complex moment invariants. *Pattern Recogn. Lett.* **26**(8), 1128–1138 (2005)
14. Liu, S., Wang, H., Wang, J., Cho, S., Pan, C.: Automatic blur-kernel-size estimation for motion deblurring. *Vis. Comput.* **31**(5), 733–746 (2015)
15. Pedone, M., Flusser, J., Heikkilä, J.: Blur invariant translational image registration for N -fold symmetric blurs. *IEEE Trans. Image Process.* **22**(9), 3676–3689 (2013)
16. Pedone, M., Flusser, J., Heikkilä, J.: Registration of images with N -fold dihedral blur. *IEEE Trans. Image Process.* **24**(3), 1036–1045 (2015)
17. Xiao, B., Ma, J.F., Cui, J.T.: Combined blur, translation, scale and rotation invariant image recognition by Radon and pseudo-Fourier-Mellin transforms. *Pattern Recogn.* **45**, 314–321 (2012)
18. Xue, F., Blu, T.: A novel SURE-based criterion for parametric PSF estimation. *IEEE Trans. Image Process.* **24**(2), 595–607 (2015)
19. Zhang, W., Cham, W.K.: Single-image refocusing and defocusing. *IEEE Trans. Image Process.* **21**(2), 873–882 (2012)
20. Zhang, Z., Klassen, E., Srivastava, A.: Gaussian blurring-invariant comparison of signals and images. *IEEE Trans. Image Process.* **22**(8), 3145–3157 (2013)